

Enhanced Saturation Coverages in Adsorption-Desorption Processes

Paul R. Van Tassel¹, Pascal Viot², Gilles Tarjus²,
Jeremy J. Ramsden³ and Julian Talbot⁴

¹*Department of Chemical Engineering and Materials Science,
Wayne State University, Detroit, MI 48202*

²*Laboratoire de Physique Théorique des Liquides
Université Pierre et Marie Curie
4, place Jussieu 75252 Paris Cedex 05 France*

³*Department of Biophysical Chemistry, Biozentrum, CH-4056 Basle, Switzerland*

⁴*Department of Chemistry and Biochemistry,
Duquesne University, Pittsburgh, PA 15282-1503*

Abstract

Many experimental studies of protein deposition on solid surfaces involve alternating adsorption/desorption steps. In this paper, we investigate the effect of a desorption step (separating two adsorption steps) on the kinetics, the adsorbed-layer structure, and the saturation density. Our theoretical approach involves a density expansion of the pair distribution function and an application of an interpolation formula to estimate the saturation density as a function of the density at which the desorption process commences, ρ_1 , and the density of the depleted configuration, ρ_2 . The theory predicts an enhancement of the saturation density compared with that of a simple, uninterrupted RSA process and a maximum in the saturation density when $\rho_2 = \frac{2}{3}\rho_1$. The theoretical results are in qualitative and in semi-quantitative agreement with the results of numerical simulations.

I. INTRODUCTION

The adsorption of proteins and colloids from solution onto solid surfaces often involves strong departure from equilibrium behavior [1]. Many experimental studies have attempted to quantify the kinetics [2–5] of the adsorption process, as well as the structure of the adsorbed configurations [6,7]. Protein adsorption has also been the subject of a number of theoretical studies. In particular, the Random Sequential Adsorption (RSA) model [8] is able to account for a number of experimentally observed properties of protein adsorption, such as irreversibility and non-linear surface blockage [9,?,?]. Quantitative expressions are now available for the kinetics of RSA of spherical [10–12] and non-spherical particles [13,14] on planar interfaces and these models have been shown to provide an excellent description of the adsorption of proteins [9,4,12], colloids [14,15] and other particles. More recently, the RSA models have been extended to allow for the possibility of post-adsorption conformational change [16,?].

It has been observed experimentally that a fraction of the proteins in an adsorbed layer may be removed by rinsing with a buffer solution or by eluting with a surfactant solution [18,19,2,3,20,21]. The influence of a desorption step on subsequent adsorption is not well understood. In particular, one would like to know how the structure of the adsorbed layer is affected by the desorption process and how this influences the kinetics when adsorption resumes. One anticipates, due to the non-equilibrium nature of the adsorption, that the intermediate desorption step may result in behavior that differs non-trivially from an uninterrupted process. It is the goal of this work to investigate this by considering a multistep RSA process that begins with the irreversible adsorption of spherical particles onto a planar surface up to a density ρ_1 . Adsorbed particles are then removed randomly until the density falls to ρ_2 . We then initiate a second irreversible adsorption process beginning from the depleted configuration and investigate how the final saturation density depends on ρ_1 and ρ_2 . The memory effect of the RSA process is expected to result in a final density that is different from that of an uninterrupted RSA process.

In the theoretical part of the study, we use a distribution function approach to determine the influence of the multistep adsorption process on the structure of the adsorbed particle configuration. A density expansion of the pair distribution function leads to an approximate description of the structure up to the maximum density in the initial adsorption step. We then show that if particles desorb randomly from the adsorbed configuration, the radial distribution function is unchanged. We use this result to estimate the available surface function of the configurations generated by the re-adsorption process and develop approximate interpolant formulas that allow us to estimate the final saturation density. The theory is then compared with numerical simulations of the process in one and two dimensions. Finally, we use these expressions to determine the extent of desorption needed to optimize the time required to reach a given adsorbed density.

II. THEORY

We consider a three-step adsorption/desorption/re-adsorption process. The initial phase consists of the irreversible addition of spherical particles of diameter σ on an initially empty planar interface to a density $\rho_1 < 0.547$ (in this work we will use ρ to denote a dimensionless

density, $\rho = \frac{\pi}{4}\sigma^2 N/A$ where N is the number of particles adsorbed in an area A). During this phase the particles are placed according to the usual RSA rules i.e., a trial position is selected from a uniform random distribution. If the trial particle does not overlap with any previously placed particles it is accepted and remains permanently fixed. Otherwise it is rejected. In the subsequent desorption step, particles in the adsorbed configuration are removed at random until the final density is ρ_2 . In the final step, the irreversible adsorption process is resumed. New particles can be added to the depleted configuration until the jamming limit is reached. As a result of the inherent memory of the RSA process, the coverage in this final state, $\rho_\infty(\rho_1, \rho_2)$ is, in general, different from the usual jamming limit for RSA that occurs without the intermediate desorption step, namely 0.547 [8].

The adsorbed configurations are characterized by a set of distribution functions $\rho_n(\mathbf{r}_1, \mathbf{r}_2, \dots, \mathbf{r}_n; \rho)$, which represent the density of finding n unspecified particles among N particles defining the system, at the positions $\mathbf{r}_1, \mathbf{r}_2, \dots, \mathbf{r}_n$ within an area A such that $\rho = N/A$. Centered on each pre-adsorbed particle is a circular exclusion region of diameter σ into which it is impossible to insert the center of an additional particle. The probability of finding a cavity of diameter 2σ centered on \mathbf{r}_1 that is free from the centers of pre-adsorbed particles is related to the distribution functions via

$$\Phi(\mathbf{r}_1^0) = 1 + \rho \int d2 f_{12} + \frac{1}{2!} \int d2 d3 f_{12} f_{13} \rho^{(2)}(2, 3, \rho) + \frac{1}{3!} \int d2 d3 d4 f_{12} f_{13} f_{14} \rho^{(3)}(2, 3, 4, \rho) + \dots \quad (1)$$

where $d1$ is shorthand for $d\mathbf{r}_1$ etc., and $f_{ij} \equiv f(r_{ij}) = \exp(-u(r_{ij})/kT) - 1$ is the Mayer function. When the interparticle potential, $u(r_{ij})$, is taken for non-overlapping hard spheres of diameter σ , the Mayer function becomes:

$$f(r_{ij}) = \begin{cases} -1, & r_{ij} < \sigma \\ 0, & r_{ij} > \sigma \end{cases} \quad (2)$$

Equation 1 applies to any configuration, equilibrium or not, of spherical particles.

Our strategy is to determine the relationship between the configurations before and after the desorption process. This allows us to find an approximate expression for Φ which we can use to estimate the saturation coverage as a function of ρ_1 and ρ_2 .

A. Initial Adsorption

The kinetics during the irreversible adsorption phase are given by

$$\frac{d\rho}{dt} = k_a \Phi \quad (3)$$

where k_a is the adsorption rate constant.

To solve for the kinetics, one writes down a hierarchy of rate equations for the distribution functions [10,11]. In particular, the pair density evolves according to

$$\frac{\partial \rho^{(2)}(1, 2, \rho)}{\partial t} = 2k_a \Phi(1, 2^o) \quad (4)$$

where $\Phi(1, 2^\circ)$ is the probability density function associated with finding an unspecified particle at \mathbf{r}_1 and a cavity of diameter 2σ free from particle centers at \mathbf{r}_2 . This function may also be expressed in terms of Mayer functions and the n-particle density functions:

$$\Phi(1, 2^\circ) = (1 + f_{12})[\rho + \int d3 f_{23}\rho^{(2)}(1, 3, \rho) + O(\rho^3)] \quad (5)$$

Substituting (3) in (4) to remove the time dependence and noting that $\rho^{(2)}(1, 3, \rho) = \rho^2(1 + f_{13})(1 + O(\rho^2))$ yields

$$\begin{aligned} \frac{\partial \rho^{(2)}(1, 2, \rho)}{\partial \rho} &= \frac{\Phi(1, 2^\circ)}{\Phi(1^\circ)} \\ &= \frac{2(1 + f_{12})[\rho + \rho^2 \int d3 f_{23}(1 + f_{13}) + O(\rho^3)]}{1 + \rho \int d2 f_{12} + O(\rho^2)} \\ &= 2(1 + f_{12})[\rho + \rho^2 \int d3 f_{13}f_{23} + O(\rho^4)] \end{aligned} \quad (6)$$

Integrating between 0 and ρ gives the pair density function to third order in ρ^3 :

$$\rho^{(2)}(1, 2, \rho) = (1 + f_{12})[\rho^2 + \frac{2}{3}\rho^3 \int d3 f_{13}f_{23} + O(\rho^4)] \quad (7)$$

B. Desorption

The subsequent desorption process results in the removal of a fraction of the particles from an initial configuration at a density ρ_1 so that the final density is ρ_2 . During this step, the density evolves according to

$$\frac{d\rho}{dt} = -k_d\rho \quad (8)$$

where k_d is the desorption constant and, if no other relaxation processes (such as surface diffusion) are operative during the desorption, the pair density function evolves according to

$$\frac{\partial \rho^{(2)}(1, 2; \rho_1, \rho)}{\partial t} = -2k_d\rho^{(2)}(1, 2; \rho_1, \rho) \quad (9)$$

where we indicate explicitly the dependence of the pair density on the density prior to desorption, ρ_1 . It follows from these two equations that

$$\frac{\partial \rho^{(2)}(1, 2; \rho_1, \rho)}{\partial \rho} = \frac{2}{\rho}\rho^{(2)}(1, 2; \rho_1, \rho) \quad (10)$$

Integrating between the initial (ρ_1) and final densities (ρ_2) yields

$$\frac{\rho^{(2)}(1, 2; \rho_1, \rho_2)}{\rho^{(2)}(1, 2; \rho_1, \rho_1)} = \frac{\rho_2^2}{\rho_1^2} \quad (11)$$

or

$$g^{(2)}(1, 2, \rho_1) = g^{(2)}(1, 2, \rho_1, \rho_1) = g^{(2)}(1, 2, \rho_1, \rho_2) \quad (12)$$

where $\rho^{(2)}(1, 2, \rho) = \rho^2 g^{(2)}(1, 2, \rho)$ defines the radial distribution function. This physically intuitive result implies that the structure of an arbitrary configuration is not altered by desorption, as long as the particles desorb randomly. Further consequences of this result and its connection with quenched annealed systems are discussed elsewhere [22].

C. Re-Adsorption

We now wish to relate the properties of configurations during the re-adsorption step to those of the configurations in the initial adsorption step. Up to third order in density, the differences between the two configurations come from the term $\rho^{(2)}(1, 2, \rho)$.

Integrating (6) between ρ_2 and $\rho > \rho_2$,

$$\rho^{(2)}(1, 2; \rho_1, \rho_2, \rho) = \rho^{(2)}(1, 2; \rho_1, \rho_2, \rho_2) + (1 + f_{12})(\rho^2 + \rho_2^2) + (1 + f_{12})\left(\frac{2}{3}\rho^3 - \frac{2}{3}\rho_2^3\right) \int d3 f_{23}f_{13} + O(\rho^4) \quad (13)$$

Using (11) to relate the pre- and post-desorption pair distribution functions, we find

$$\rho^{(2)}(1, 2; \rho_1, \rho_2, \rho) = (1 + f_{12})\left[\rho^2 + \frac{2}{3}[\rho^3 + \rho_2^2(\rho_1 - \rho_2)] \int d3 f_{13}f_{23} + O(\rho^4)\right] \quad (14)$$

Substituting in (1) then yields

$$\Phi(\rho_1, \rho_2, \rho) = 1 + \rho \int d2 f_{12} + \frac{1}{2}\rho^2 \int d2 d3 (1 + f_{23}) \quad (15)$$

$$+ \frac{1}{3}[\rho^3 + \rho_2^2(\rho_1 - \rho_2)] \int d2 d3 d4 f_{12}f_{13}f_{24}f_{34}(1 + f_{23}) \quad (16)$$

$$+ \frac{1}{6}\rho^3 \int d2 d3 d4 f_{12}f_{13}f_{14}(1 + f_{23})(1 + f_{24})(1 + f_{34}) + O(\rho^4) \quad (17)$$

$$= \Phi^{\text{RSA}}(\rho) + A_{32}\rho_2^2(\rho_1 - \rho_2), \quad \rho \geq \rho_2 \quad (18)$$

where

$$A_{32} = \frac{128}{3\pi^2} \left(\frac{\pi\sqrt{3}}{2} - \frac{9}{4} \right) \quad (19)$$

is the portion of the 3rd order RSA coefficient due to first order corrections of $g^{(2)}$ [10]. We note that $\Phi(\rho_1, \rho_2, \rho)$ correctly reduces to $\Phi^{\text{RSA}}(\rho)$ in both the limit where $\rho_1 = \rho_2$ (no desorption) and $\rho_2 = 0$ (total desorption).

During desorption, it is easy to show that

$$\Phi(\rho_1, \rho) = \Phi^{\text{RSA}}(\rho) + A_{32}\rho^2(\rho_1 - \rho) + O(\rho^3), \quad \rho_1 \geq \rho \geq \rho_2 \quad (20)$$

We plot that Φ during adsorption, Φ^{RSA} , desorption $\Phi(\rho_1, \rho)$, and re-adsorption, $\Phi(\rho_1, \rho_2, \rho)$, in Fig. VII. One can also show that

$$\left. \frac{d\Phi}{d\rho} \right|_{1,\text{ads}} = \left. \frac{d\Phi}{d\rho} \right|_{1,\text{des}} + A_{32}\rho_1^2 \quad (21)$$

where the subscripts ads and des indicate the adsorption and desorption branches, respectively and since $A_{32} > 0$, we have

$$\left. \frac{d\Phi}{d\rho} \right|_{1,\text{ads}} > \left. \frac{d\Phi}{d\rho} \right|_{2,\text{des}} \quad (22)$$

so the slope of Φ during desorption is more negative. One has, furthermore, that

$$\left. \frac{d\Phi}{d\rho} \right|_{2,\text{ads}} = \left. \frac{d\Phi}{d\rho} \right|_{2,\text{des}} - A_{32}\rho_2(2\rho_1 - 3\rho_2) \quad (23)$$

so

$$\left. \frac{d\Phi}{d\rho} \right|_{2,\text{ads}} > \left. \frac{d\Phi}{d\rho} \right|_{2,\text{des}}, \quad \rho_2 < \frac{2}{3}\rho_1 \quad (24)$$

$$\left. \frac{d\Phi}{d\rho} \right|_{2,\text{ads}} < \left. \frac{d\Phi}{d\rho} \right|_{2,\text{des}}, \quad \rho_2 > \frac{2}{3}\rho_1 \quad (25)$$

and thus the change in Φ may be more pronounced in either desorption or re-adsorption. It is clear that in either case, the available surface function is enhanced compared with the simple RSA value (at least to third order in density) since

$$\Phi(\rho_1, \rho_2, \rho) - \Phi^{\text{RSA}}(\rho) = A_{32}\rho_2^2(\rho_1 - \rho_2) > 0, \quad \rho > \rho_2 \quad (26)$$

To obtain quantitative results, we consider the interpolation formula

$$\Phi(\rho_1, \rho_2, \rho) = [1 + A_{32}\rho_2^2(\rho_1 - \rho_2)](1 - x)^3(1 + a_1x + a_2x^2) \quad (27)$$

where

$$x = \rho/\rho_\infty \quad (28)$$

This form is consistent with the asymptotic kinetics,

$$\rho_\infty - \rho \sim t^{-1/2} \quad (29)$$

Finally, (27) correctly reduces to the equation used to determine ρ_∞ for simple RSA when $\rho_1 = \rho_2$ or when $\rho_2 = 0$. Expanding the interpolant in powers of ρ and equating the coefficients with those of (1) yields an estimate for $\rho_\infty(\rho_1, \rho_2)$. As can be seen in Figure VII, the saturation coverage is a monotonically increasing function of ρ_1 and exhibits a maximum versus ρ_2 . Actually, the saturation density increases monotonically with the combination $\rho_2^2(\rho_1 - \rho_2)$, so a maximum occurs for $\rho_2 = (2/3)\rho_1$.

In one dimension, the coefficient A_{32} takes the value $2/9$. Unfortunately, however, the analogous interpolation formula, $\Phi(\rho) = [1 + A_{32}\rho_2^2(\rho_1 - \rho_2)](1 - x)^2(1 + a_1x + a_2x^2)$ does not yield physically acceptable estimates of the jamming density, even in the simple RSA case.

III. SIMULATION

The adsorption-desorption process was simulated using techniques that have been described previously. Disks are deposited randomly and uniformly in a periodic cell of area A , subject to the usual RSA constraints of no overlap and no desorption, until the coverage reaches the preset value, ρ_1 . In the desorption step, randomly selected particles are removed until the coverage falls to ρ_2 . The RSA process is then restarted and continued for a total of N_{trial} attempts. In this way we obtain the time-dependent coverage, $\rho(t)$, where $t = a_{\text{rel}}i$, $a_{\text{rel}} = \pi\sigma^2/4A$ and i is the number of attempts that have been made. This function is then averaged over a number, N_{av} , of independent runs. The coverage in the jamming limit was estimated by assuming that at long times the kinetics are described by the usual asymptotic kinetics, (29).

The simulation procedure in one-dimension is somewhat different. Rods of unit length are deposited randomly on a line of length L subject to the usual constraints of no overlap and no desorption. When the jamming limit coverage is nearly reached, all the remaining available gaps, each of which can by now accommodate at most one additional rod, are filled by inserting rods randomly and uniformly within them. Partial desorption is then simulated by looping through all the adsorbed particles and removing each with a probability p_{des} . This is achieved by generating a uniform random number between zero and one. If this number is less than p_{des} the particle is removed. The depleted configuration then serves as the initial configuration for a new irreversible adsorption process which continues until jamming. If N denotes the number of adsorbed rods, then the coverage is computed from $\rho = N/(L - 1)$. Since the jamming limit can be reached exactly in the one-dimensional system, the final results are expected to be more accurate than in two dimensions.

IV. RESULTS

In both one and two dimensions, the new jammed state has a higher coverage than that of simple RSA, although the effect is smaller than predicted by the theory. In one dimension, Figure VII shows that the maximum density (just over 0.78) occurs for $p_{\text{des}} \approx 0.4$ or $\rho_2 \approx 0.6$, which is consistent with, although a little larger than, the theoretical prediction of $\rho_2 = (2/3)\rho_1$.

In two dimensions (Figure VII), the enhancement is not statistically significant for $\rho_1 = 0.4$. For $\rho_1 = 0.53$ the effect is clearly evident and the maximum final coverage occurs for $\rho_2 \approx 0.4$ while the theoretical estimate is 0.353.

That the theory overestimates the enhancement is not totally surprising. The estimate of the saturation coverage provided by the interpolation formula for simple RSA (0.553) exceeds the actual value (0.547). Moreover, the pair density function is taken only to second order in ρ .

V. APPLICATION

An interesting consequence of the findings of this article is that it may be possible to achieve a given surface coverage using an intervening desorption process in a shorter time

than with a continuous adsorption process. We can readily quantify this idea by minimizing the time required to reach a given surface coverage in an adsorption-desorption-adsorption process by optimizing densities at which the desorption step begins, ρ_1 , and ends, ρ_2 . Let t_f denote the time at which the adsorbed density is ρ_f . In a process with a single desorption step

$$t_f = t_{\text{ads}} + t_{\text{des}} + t_{\text{reads}} \quad (30)$$

$$= \int_0^{\rho_1} [\Phi^{RSA}(\rho)]^{-1} d\rho + \int_{\rho_1}^{\rho_2} [k_d \rho]^{-1} d\rho + \int_{\rho_2}^{\rho_f} [\Phi(\rho_1, \rho_2, \rho)]^{-1} d\rho \quad (31)$$

We find the minimum time to reach the density ρ_f by by optimizing the density at the beginning of the desorption step and that after desorption. As we will demonstrate, the amount adsorbed in such a process can exceed that in a continuous adsorption process without interruption. The required densities are found from a numerical solution of the equations

$$\frac{\partial t_f}{\partial \rho_1} = 0 \quad (32)$$

$$\frac{\partial t_f}{\partial \rho_2} = 0 \quad (33)$$

This is achieved by iterating the following matrix equation:

$$\begin{bmatrix} \rho_1 \\ \rho_2 \end{bmatrix}^{\text{new}} = \begin{bmatrix} \rho_1 \\ \rho_2 \end{bmatrix} - \begin{bmatrix} \frac{\partial^2 t_f}{\partial \rho_1^2} & \frac{\partial^2 t_f}{\partial \rho_1 \partial \rho_2} \\ \frac{\partial^2 t_f}{\partial \rho_1 \partial \rho_2} & \frac{\partial^2 t_f}{\partial \rho_2^2} \end{bmatrix}^{-1} \begin{bmatrix} \frac{\partial t_f}{\partial \rho_1} \\ \frac{\partial t_f}{\partial \rho_2} \end{bmatrix}$$

The calculations were performed using an interpolation formula,

$$\Phi^{RSA}(\rho) = (1 - x)^3(1 + b_1 x + b_2 x^2 + b_3 x^3) \quad (34)$$

where $x = \rho/\rho_\infty$ and b_1 , b_2 , and ρ_∞ are taken from reference [10]. Fig. VII shows ρ_1 and ρ_2 which minimize the time required to produce an adsorbed configuration with a final density of ρ_f . For a given value of k_d , the two curves converge at ρ_{f0} . If the desired final density is larger than this value, it will be more efficient i.e., require less time, with a two-step process than with a single step process. If the final density is less than ρ_{f0} , the single step process is more efficient. As k_d increases, ρ_{f0} decreases since the time required to remove a given fraction of particles is a decreasing function of k_d . Thus at large desorption rates less time is spent in the desorption phase. We observe that ρ_1 appears to be almost independent of k_d (for $\rho_f > \rho_{f0}$), while ρ_2 curves converge at large values of k_d . The two-step process is most efficient in the limit $k_d \rightarrow \infty$. That the two step process can be more efficient than a one-step process is a result of the inherent memory of the adsorbed configurations. Without this memory effect, the two-step process is always less efficient.

VI. CONCLUSION

We have developed a theoretical approach for modeling a three-step surface filling process composed of two irreversible adsorption steps separated by a desorption step. This approach

considers the effects of surface density and coverage history on the adsorbate particle distribution functions and predicts an enhancement of the saturation surface density that is maximized when one third of the molecules are removed during the intermediate desorption step.

One experimental realization of this process is partially reversible macromolecular adsorption where only a certain fraction of molecules desorb during a buffer rinse. Partial reversibility may be due to adsorbent heterogeneity, formation of stable clusters of molecules on the surface, or post-adsorption transitions in conformation or orientation. Another experimental realization of this process is the elution of otherwise irreversibly adsorbed macromolecules with surfactant or detergent eluting agents [21]. The results presented here could have important implications for these and other multi-step filling processes when a high saturation density and/or a rapid surface filling is required.

VII. ACKNOWLEDGMENTS

P. R. Van Tassel thankfully acknowledges a NATO-NSF Postdoctoral Fellowship. J. Talbot and P. R. Van Tassel thank the NSF for financial support. The Laboratoire de Physique Théorique des Liquides is a Unité Mixte de Recherche no. 7600 associated with the Centre National de la Recherche Scientifique.

REFERENCES

- [1] J. D. Andrade and V. Hlady, *Adv. Polymer Sci.*, **86**, 1 (1986)
- [2] M. Wahlgren, T. Arnebrant and I. Lundström, *J. Coll. Int. Sci.*, **175** 506, (1995)
- [3] J. Buijs, P. A. W. Van den Berg, J. W. Th. Lichtenbelt, W. Norde and J. Lyklema, *J. Coll. Int. Sci.*, **178**, 594 (1996)
- [4] J. J. Ramsden, *J. Stat. Phys.*, **73**, 853 (1993)
- [5] J. L. Robeson and R. D. Tilton, *Langmuir*, **12**, 6104 (1996)
- [6] Z. Adamczyk, B. Siwek, M. Zembala and P. Belouschek, *Adv. Colloid Interface Sci.* **48**, 151 (1994)
- [7] D. C. Cullen and C. R. Lowe, *J. Colloid Interface Sci.*, **166**, 102 (1994)
- [8] J. W. Evans, *Rev. Mod. Phys.*, **65**, 1281 (1993)
- [9] J. J. Ramsden, *Phys. Rev. Lett.*, **71**, 295 (1993)
- [10] P. Schaaf and J. Talbot, *Phys. Rev. Lett.* **62**, 175 (1989); *J. Chem. Phys.*, **91**, 4401 (1989)
- [11] G. Tarjus, P. Schaaf and J. Talbot, *J. Stat. Phys.*, **63**, 167 (1991)
- [12] X. Jin, Ph.D. thesis, Purdue University (1994)
- [13] S. M. Ricci, J. Talbot, G. Tarjus and P. Viot, *J. Chem. Phys.*, **97**, 5219 (1992)
- [14] Z. Adamczyk, B. Siwek, M. Zembala and P. Weronki, *J. Chem. Phys.*, **105**, 5562 (1996)
- [15] P. R. Johnson and M. Elimelech, *Langmuir*, **11**, 801 (1995)
- [16] P. R. Van Tassel, P. Viot, G. Tarjus and J. Talbot *J. Chem. Phys.*, **91**, 7064 (1994)
- [17] P. R. Van Tassel, J. Talbot, G. Tarjus and P. Viot, *Phys. Rev. E*, **53**, 785 (1996)
- [18] R. Kurrat, J.J. Ramsden and J.E. Prenosil, *J. Chem. Soc.* **90**, 587 (1994)
- [19] K. Wannerberger and T. Arnebrant, *J. Colloid Interface Sci.*, **177**, 316 (1996)
- [20] M. Malmsten, B. Lassen, J. Westin, C.-G. Golander, R. Larson and U.R. Nilsson, *J. Colloid Interface Sci.*, **179**, 163 (1996)
- [21] M. Wahlgren, S. Welin-Klintström and C. A.-C. Karlsson, 485, *Biopolymers at Interfaces*, M. Malmsten ed. Marcel Dekker, New York (1998)
- [22] P. R. Van Tassel, J. Talbot, P. Viot and G. Tarjus *Phys. Rev. E*, **56**, R1299 (1997)
- [23] R. D. Tilton, C. R. Robertson, A. P. Gast, *J. Colloid Inteface Sci.*, **137**, 192 (1989)
- [24] W. Norde and A. C. I. Ausiem, **66**, 73 (1992)

FIGURES

FIG. 1. The available surface function plotted as a function of density at various fixed densities prior to and following desorption. The bottom line is properly placed and each subsequent line is shown displaced vertically by 0.1 units for clarity.

FIG. 2. The jamming limit density, as determined from the interpolation formula (27), as a function of (a) the density, ρ_1 at which desorption begins and (b) the density, ρ_2 , at which desorption ends.

FIG. 3. Enhancement of the jamming limit coverage, ρ_f , in one dimension resulting from a random desorption from a jamming RSA configuration of hard rods on a line. Each particle is desorbed from this configuration with probability p_{des} before re-adsorption to a new jamming limit.

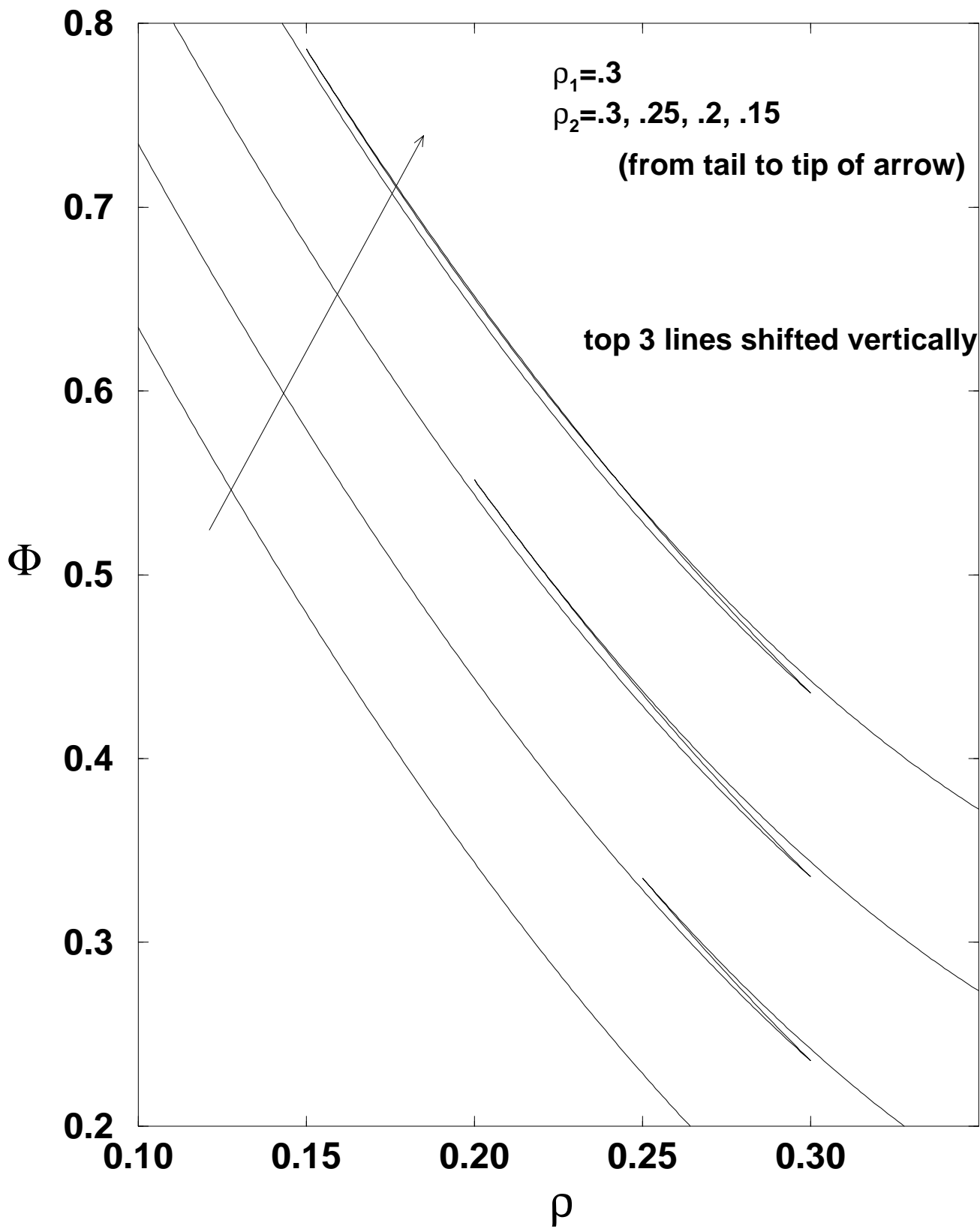
FIG. 4. Enhancement of the jamming limit coverage, ρ_f , in two dimensions resulting from a random desorption at a density ρ_1 to a density ρ_2 as determined in a numerical simulation of the process. +: $\rho_1 = 0.53$, *: $\rho_1 = 0.5$, diamonds: $\rho_1 = 0.4$.

FIG. 5. Kinetics of an adsorption-desorption-adsorption process. (a) For a given desorption rate, k_d , the values of the densities ρ_1 and ρ_2 that minimize the time required to reach the final coverage ρ_f . (b) Comparison of the optimized two step process with $k_d = 1$ and optimized for $\rho_f = 0.5$ with an uninterrupted adsorption process. Note that the final coverage is attained more rapidly using the two-step process.

TABLES

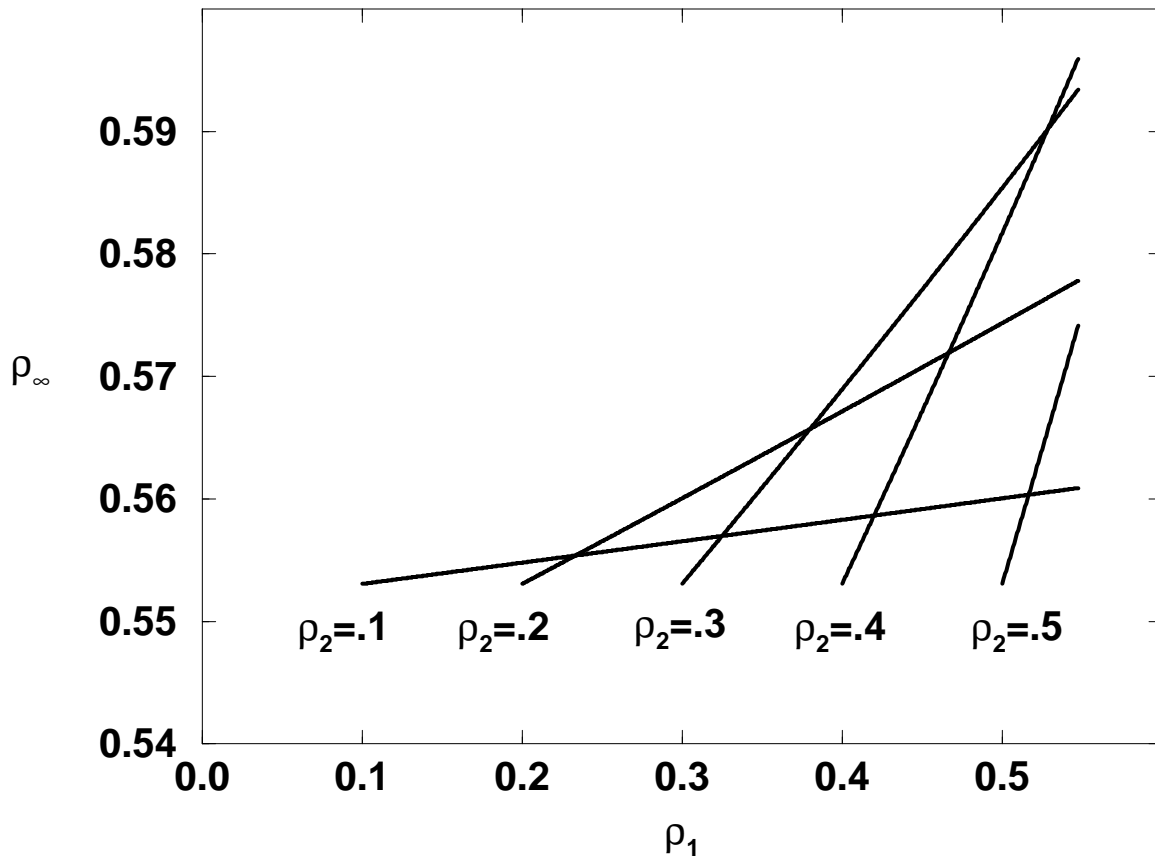
TABLE I. Enhancement of the Saturation Coverage. Particles are desorbed randomly from an RSA configuration at an initial density ρ_1 until the density reaches ρ_2 . A new RSA process then begins on the depleted configuration. The density at saturation is then estimated by extrapolating the coverage versus time curves using the asymptotic power law, (29). Each condition used 800 independent averages for a system with a relative area of the particle to simulation cell of 0.001. For $\theta_1 = 0.53$ a total of 10^7 attempts were made to add new particles, while for $\theta_1 = 0.50$ and $\theta_1 = 0.4$ we used 5×10^6 attempts.

ρ_1	ρ_2	ρ_∞
0.53	0.05	0.5474
	0.10	0.5486
	0.15	0.5500
	0.20	0.5511
	0.25	0.5524
	0.30	0.5539
	0.35	0.5546
	0.40	0.5544
	0.45	0.5529
0.50	0.05	0.5473
	0.1	0.5477
	0.15	0.5484
	0.20	0.5496
	0.25	0.5499
	0.30	0.5504
	0.35	0.5504
	0.40	0.5503
	0.45	0.5491
0.45	0.05	0.5474
	0.10	0.5472
	0.15	0.5477
	0.20	0.5478
	0.25	0.5479
	0.30	0.5482
	0.35	0.5476
0.40	0.5473	

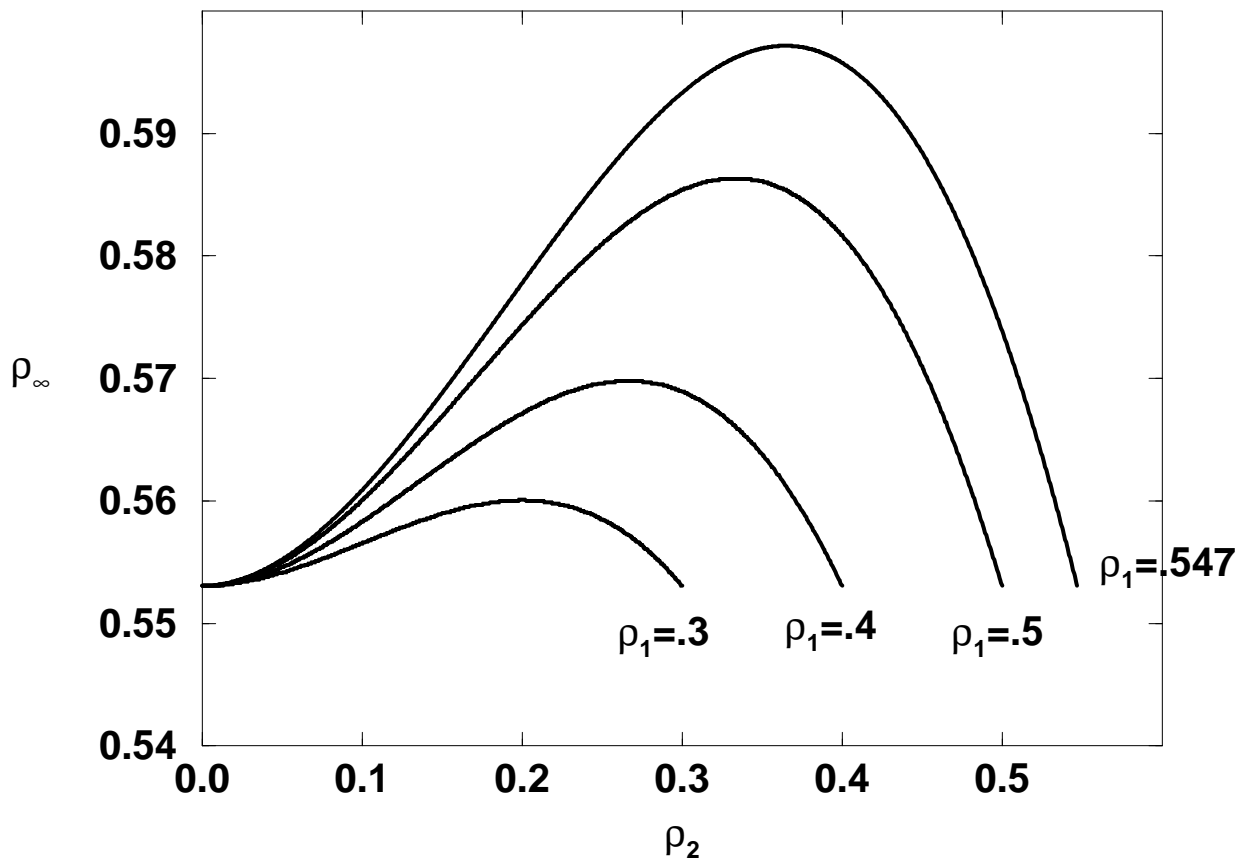


Talbot, et al, Fig. 1

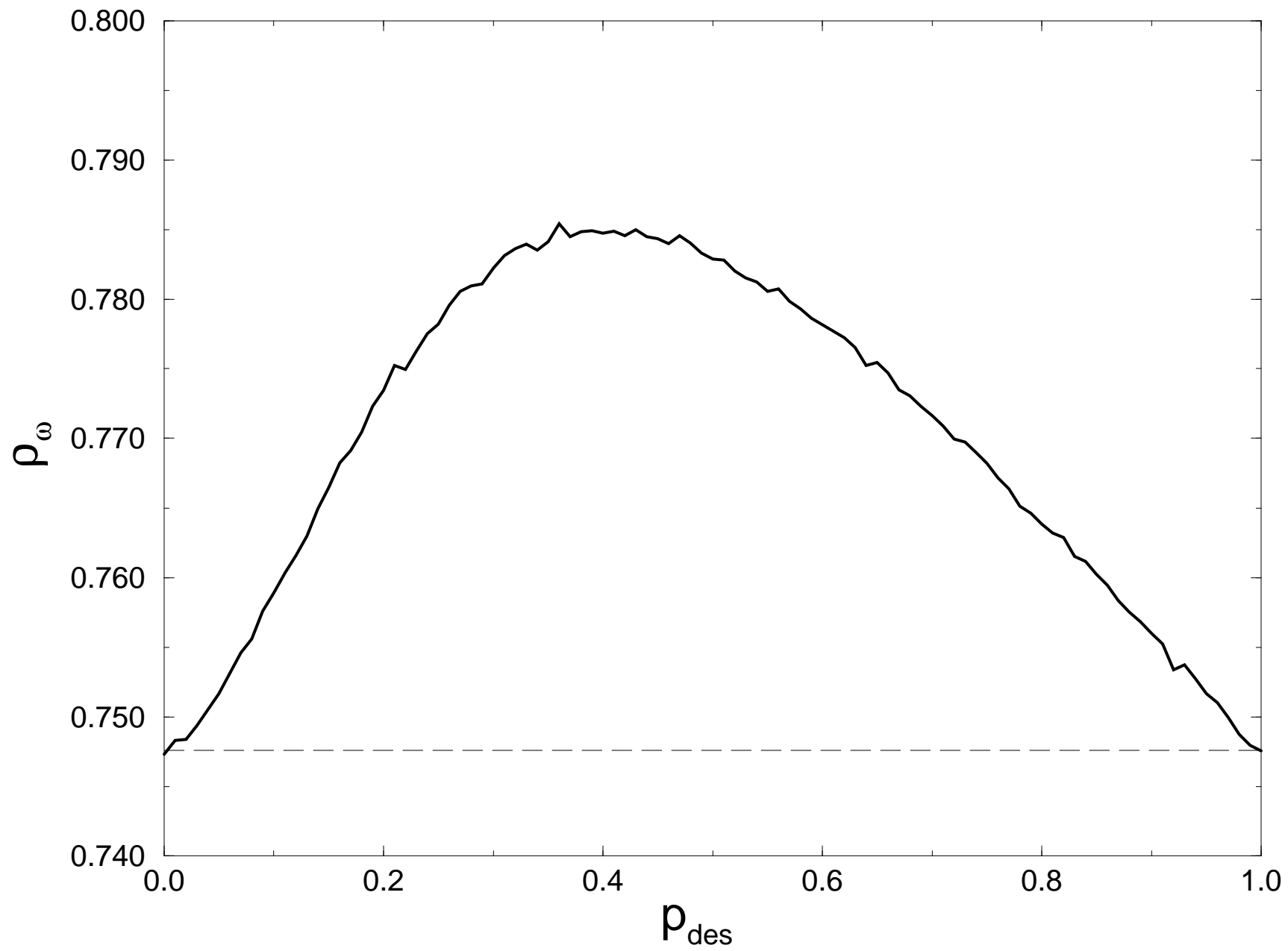
a)

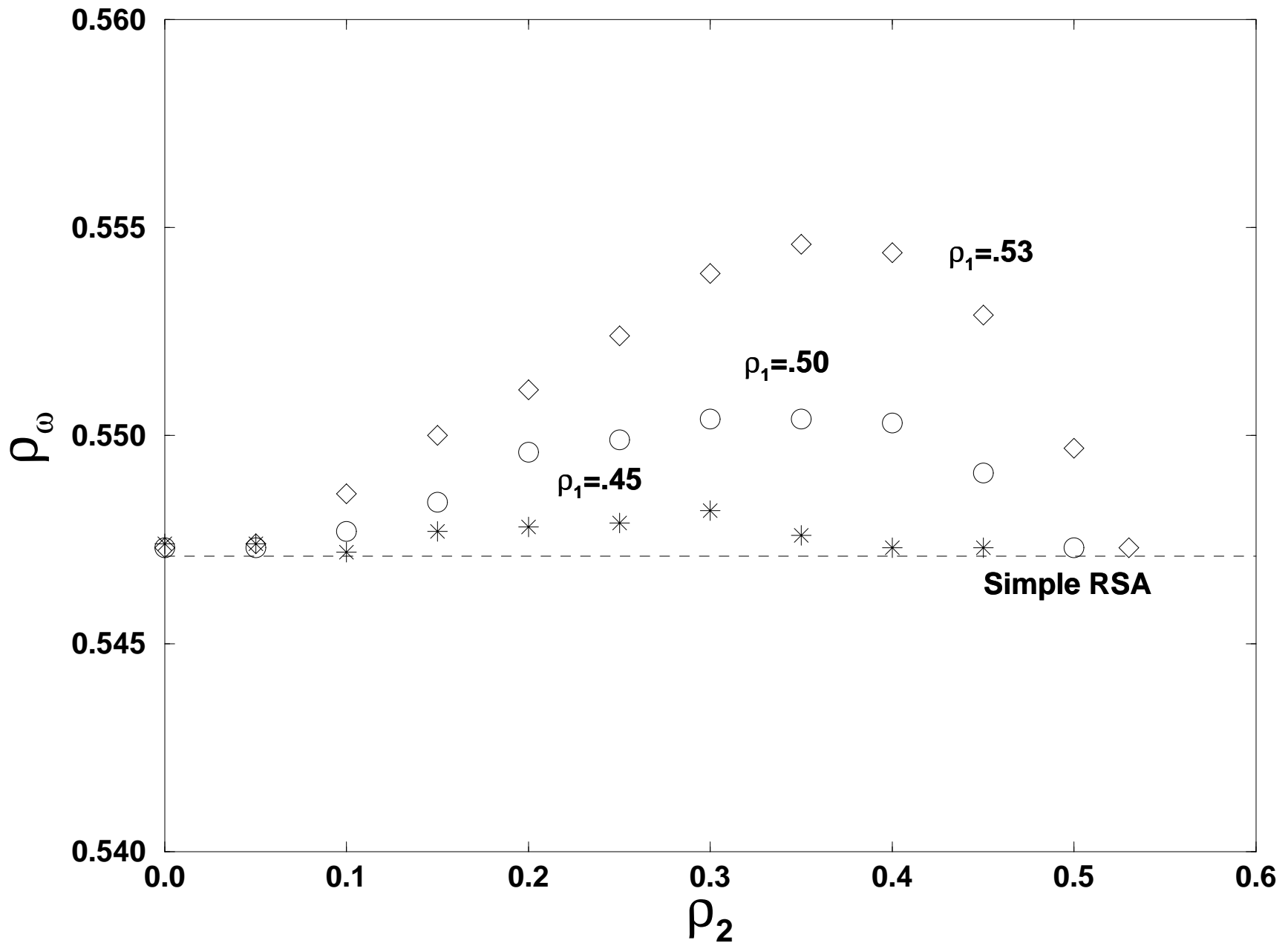


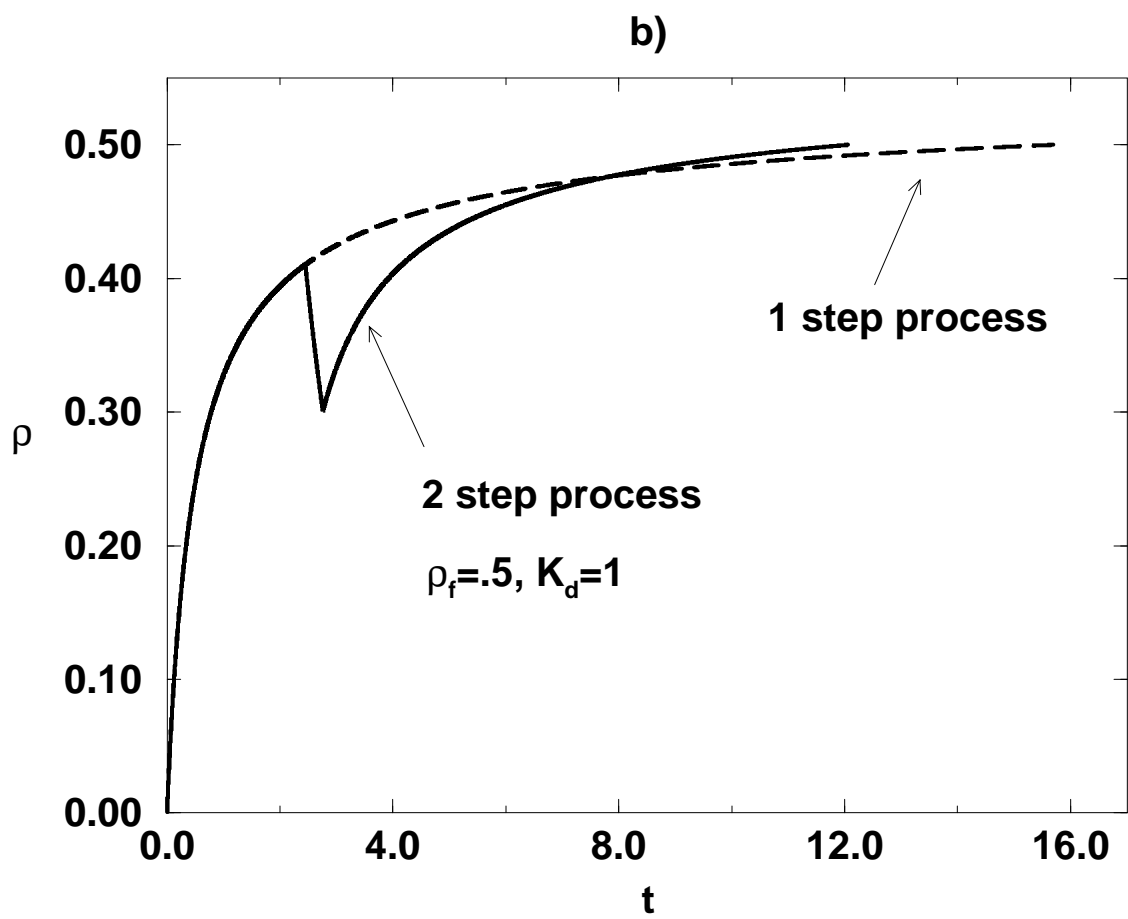
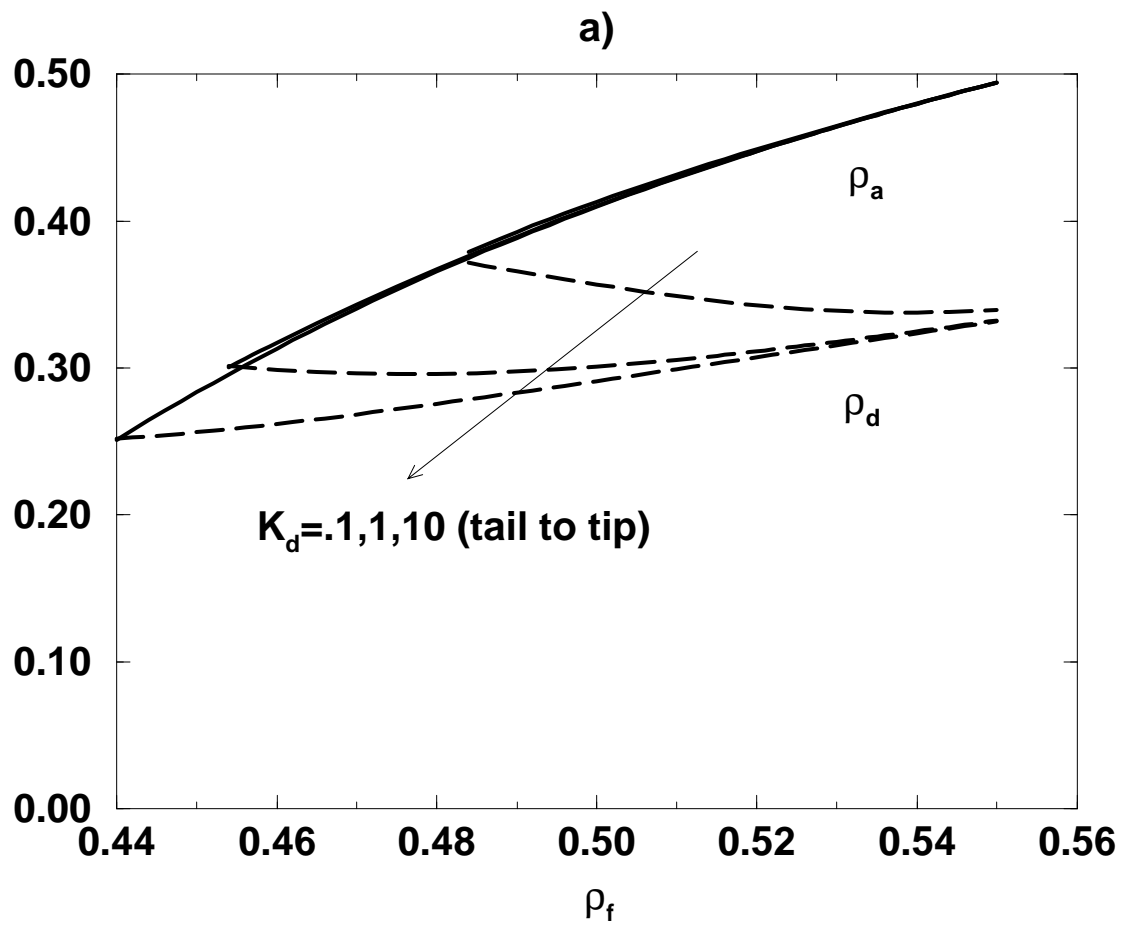
b)



Talbot, et al, Fig. 2







Talbot, et al, Fig. 5